



Estimating the timing of geophysical commitment to 1.5 and 2.0 °C of global warming

M. T. Dvorak¹✉, K. C. Armour^{1,2}, D. M. W. Frierson², C. Proistosescu^{3,4}, M. B. Baker⁵ and C. J. Smith^{6,7}

Following abrupt cessation of anthropogenic emissions, decreases in short-lived aerosols would lead to a warming peak within a decade, followed by slow cooling as GHG concentrations decline. This implies a geophysical commitment to temporarily crossing warming levels before reaching them. Here we use an emissions-based climate model (FaIR) to estimate temperature change following cessation of emissions in 2021 and in every year thereafter until 2080 following eight Shared Socioeconomic Pathways (SSPs). Assuming a medium-emissions trajectory (SSP2-4.5), we find that we are already committed to peak warming greater than 1.5 °C with 42% probability, increasing to 66% by 2029 (340 GtCO₂ relative to 2021). Probability of peak warming greater than 2.0 °C is currently 2%, increasing to 66% by 2057 (1,550 GtCO₂ relative to 2021). Because climate will cool from peak warming as GHG concentrations decline, committed warming of 1.5 °C in 2100 will not occur with at least 66% probability until 2055.

The Paris Agreement has affirmed an international goal to hold global warming to well below 2 °C and to pursue efforts to limit it to 1.5 °C relative to pre-industrial temperatures. However, global warming is projected to exceed 1.5 °C within decades and 2 °C by mid-century in all but the lowest emission scenarios¹. That is, there is limited time and allowable carbon dioxide (CO₂) emissions (a remaining carbon budget) before these temperature thresholds are exceeded. Assessing the possibility of avoiding these global warming levels requires a clear understanding of the unrealized warming that is inevitable due to past emissions (a geophysical warming commitment), treated separately from the warming associated with future, and therefore theoretically avoidable, emissions (a socioeconomic warming commitment).

In this Article, we provide a quantification of the geophysical warming commitment and its evolution over time in terms of the zero-emissions commitment (ZEC) (°C), a common metric used to estimate the global temperature change that follows an abrupt cessation of emissions. The magnitude of the ZEC depends on the evolution of atmospheric GHG concentrations and aerosol content after emissions cease, along with the multiple timescales of climate response to changes in radiative forcing. If only CO₂ emissions cease, global temperature is expected to remain relatively constant as both ocean heat uptake and atmospheric CO₂ forcing slowly decline by similar, and compensating, amounts^{2–6}. Estimates of the ZEC following a cessation of only CO₂ emissions (referred to here as ZEC_{CO₂}) range from slight cooling to continued warming^{6,7} over multiple centuries, depending on model representations of ocean heat uptake, carbon cycle, climate feedbacks and historical emissions pathways^{4,6,8–10}. On average, ZEC_{CO₂} is taken to be small throughout the twenty-first century when estimated from multimodel simulations^{1,8}. This suggests that future warming is governed primarily by future emissions rather than by past emissions, and thus society is not geophysically committed to exceeding key global warming levels before reaching them.

However, the situation becomes more complex when the emissions of short-lived climate forcers, including non-CO₂ GHGs and aerosols, are considered^{3,11,12}. Tropospheric aerosols produced through the combustion of fossil fuels and biomass burning have atmospheric lifetimes of days to weeks and currently exert a strong net cooling effect on the climate (a negative radiative forcing). Thus, the ZEC associated with the cessation of all anthropogenic emissions (ZEC_{anthro}) would include warming associated with the rapid reduction of aerosols and consequent ‘unmasking’ of a portion of GHG forcing. This warming is offset in small part by the removal of black carbon on snow (a positive surface albedo forcing) and in larger part by a decrease in tropospheric ozone, nitrous oxide and methane concentrations over the following weeks to decades, followed by a slower decline as GHG concentrations decrease until the global temperature stabilizes at a value determined by the residual forcing associated with the portion of anthropogenic CO₂ that remains in the atmosphere for millennia^{3,12,13}.

We thus focus on two measures of the climate commitment following a complete cessation of anthropogenic emissions: the peak temperature reached in the decades following emissions cessation (ZEC_{anthro}^{peak}) and the eventual temperature reached in the year 2100 (ZEC_{anthro}²¹⁰⁰). These two measures represent different aspects of committed warming that may be relevant to different components of the climate system and impacts thereupon; that is, systems that respond quickly to global temperature change would be sensitive to peak warming (for example, sea ice, the hydrological cycle, hurricanes, agriculture and many ecosystems), while those that respond slowly to global temperature change would be sensitive to long-term warming (for example, glaciers, ice sheets and sea level).

Both measures of commitment (ZEC_{anthro}^{peak} and ZEC_{anthro}²¹⁰⁰) depend on the magnitude and evolution of GHG and aerosol radiative forcing following emissions cessation, the sensitivity of climate

¹School of Oceanography, University of Washington, Seattle, WA, USA. ²Department of Atmospheric Sciences, University of Washington, Seattle, WA, USA. ³Department of Atmospheric Sciences, University of Illinois Urbana-Champaign, Champaign, IL, USA. ⁴Department of Geology, University of Illinois Urbana-Champaign, Champaign, IL, USA. ⁵Department of Earth and Space Sciences, University of Washington, Seattle, WA, USA. ⁶Priestley International Centre for Climate, University of Leeds, Leeds, UK. ⁷International Institute for Applied Systems Analysis (IIASA), Laxenburg, Austria.

✉e-mail: mtdvorak@uw.edu

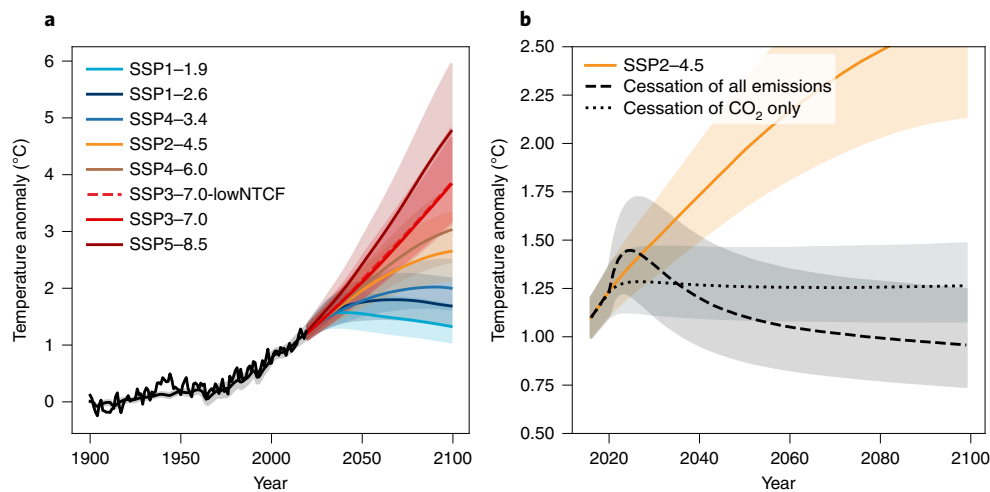


Fig. 1 | Constrained FaIR ensemble global temperature projections. **a**, Global warming following SSPs with the historical temperature record from HadCRUT5⁴¹ overlaid in black. **b**, SSP2-4.5 with no cessation of emissions (orange line), with a cessation of only CO₂ emissions (dotted line, ZEC_{CO₂}) and of all anthropogenic emissions (dashed line, ZEC_{anthro}) in the beginning of 2021. Shading represents the 66% confidence interval obtained from a 6,729-posterior-member ensemble (Methods). Global temperature anomalies are taken relative to the 1850–1900 average.

to forcing changes (often characterized in terms of the equilibrium climate sensitivity (ECS) (°C) and the timescales of climate adjustment associated with the oceans^{3,13}. Cessation of emissions from present-day levels generally results in a ZEC_{anthro}^{peak} of a few tenths of a degree Celsius above the current temperature, with an overshoot lasting approximately a decade before cooling to near-present temperatures^{13–15}. However, a larger ZEC_{anthro}^{peak} with a more prolonged overshoot is possible if aerosol forcing is strong and climate sensitivity is high^{3,15}. Thus, a full accounting of past emissions suggests that society may be geophysically committed to peak warming exceeding key global warming levels many years before those levels are reached—absent efforts to directly remove CO₂ from the atmosphere.

Recent research has substantially advanced scientific understanding of the instrumental record of global warming¹⁶, Earth's energy imbalance^{17,18}, aerosol radiative forcing^{18,19} and climate sensitivity^{18,20}. In light of these advances, the current geophysical climate commitment needs to be revisited. Furthermore, both ZEC_{anthro}^{peak} and ZEC_{anthro}²¹⁰⁰ will change over time as GHG emissions continue and the blend of radiative forcing agents in the atmosphere evolves. Key questions are when the world will be geophysically committed to reaching key global warming levels, such as 1.5 and 2.0°C, either temporarily (overshoot) or at the end of the century and how these estimates depend on the emissions trajectory.

We quantify both ZEC_{anthro}^{peak} and ZEC_{anthro}²¹⁰⁰ associated with a cessation of all anthropogenic emissions using an emissions-based climate model, Finite Amplitude Impulse Response (FaIR) model (v.1.3)^{21,22} with model parameters constrained by observations of global energy budget and temperature trends since the 1800s (Methods). FaIR produces effective radiative forcing from emissions time series of 39 gases and short-lived climate forcers, with an intermediate concentration calculation for GHGs and a four-timescale carbon-cycle representation that is sensitive to changes in uptake efficiency with cumulative emissions and temperature. Changes in land-use forcing are excluded from this analysis because it is unclear how they should be represented in the ZEC framework (for example, ref. ²³), but sensitivity tests show that including land-use forcing has little impact on the results presented here (Methods and Supplementary Fig. 1). Global temperature is calculated using a two-layer ocean model^{24,25} (Methods) that was also used for the global temperature projection assessment in the IPCC's Sixth Assessment Report (IPCC AR6)¹.

Priors for key model parameters, including the radiative feedback parameter (which governs ECS), the efficiency of ocean heat uptake, ocean effective heat capacities, the magnitude of GHG and aerosol forcing, and carbon-cycle parameters are generated to match distributions of state-of-the-art global climate models²⁵ and IPCC AR6 estimates^{18,26} (Methods and Extended Data Figs. 1–4). Posterior model parameter distributions are then selected on the basis of fits to observational records of global surface temperature, global energy accumulation and radiative forcing since 1850, as well as present-day CO₂ levels. These constraints result in a posterior FaIR model ensemble that accurately fits the historical temperature record to within an estimate of internal temperature variability (Extended Data Fig. 5) and closely matches the projections of twenty-first-century warming as assessed by IPCC AR6¹ (Fig. 1a).

Posterior estimates of ECS and the transient climate response (TCR) are 2.9°C (1.8–4.7°C, 5–95% confidence) and 1.7°C (1.2–2.5°C), respectively. Median aerosol forcing is estimated to be -1.2 W m^{-2} (-1.8 to -0.6 W m^{-2}) in 2018 relative to 1765. These values are all in good agreement with recent assessments based on multiple lines of evidence^{19,20}, including IPCC AR6¹⁸.

With the posterior FaIR ensemble, we first evaluate ZEC_{anthro}^{peak} and ZEC_{anthro}²¹⁰⁰ associated with an abrupt cessation of anthropogenic emissions near the present day (taken as January 2021) (Fig. 1b). We find a median ZEC_{anthro}^{peak} of 0.22°C relative to 2020, with an overshoot that lasts for approximately 18 years before eventually cooling to several tenths of a degree Celsius below 2020 temperatures by the end of the century (Fig. 1b, dashed line). Ref. ¹³, also using FaIR, estimated a median ZEC_{anthro}^{peak} of approximately 0.1°C above 2018, while ref. ¹⁵, using an intermediate-complexity model, found median peak warming of 0.3°C following a cessation of all emissions. This difference in results is due in large part to differences in aerosol forcing at the time of emissions cessation among ref. ¹³ (-1.4 to -0.2 W m^{-2} , 90% confidence range), ref. ¹⁵ (-1.9 to -0.8 W m^{-2}) and this study (-1.8 to -0.6 W m^{-2}), as well as larger climate sensitivity in ref. ¹⁵.

Similar to ref. ¹³, we find net cooling at the end of the century following emissions cessation (a median ZEC_{anthro}²¹⁰⁰ of -0.4 °C below the 2020 temperature), which is in contrast to the end-of-century warming of approximately 0.3°C found in a previous study¹²—a difference that may be due to different assumptions about residual GHG and non-CO₂ forcing in the ZEC experiment and the sensitivity

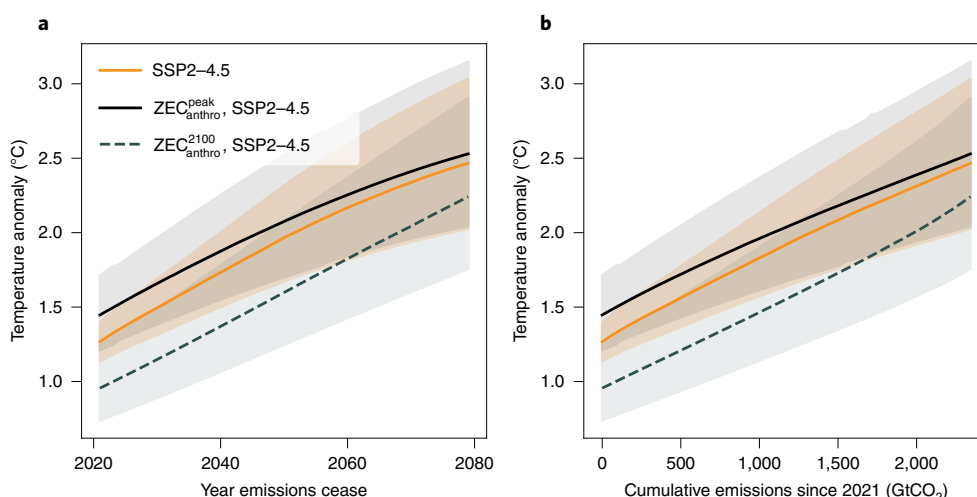


Fig. 2 | Committed warming and scenario warming following SSP2-4.5. **a, b**, FaIR ensemble temperature projections assuming no cessation of emissions (orange line) and warming commitments, ZEC_{anthro}^{peak} (solid black line) and ZEC_{anthro}^{2100} (dashed black line), as functions of emissions cessation year (**a**) and cumulative anthropogenic CO_2 emissions since the beginning of 2021 (**b**). For SSP2-4.5 in **a**, the x axis is ‘Year’. Shading indicates the 66% confidence interval. Global temperature anomalies are taken relative to the 1850–1900 average.

Table 1 | Year in which a cessation of anthropogenic emissions leads to ZEC_{anthro}^{peak} and ZEC_{anthro}^{2100} of 1.5, 1.7 and 2°C following SSP2-4.5 at the 17th, 50th, 66th and 83rd percentile confidence levels

Global warming since 1850–1900 (°C)	Temperature metric	Commitment year by ensemble percentile				
		17th	50th	66th	83rd	
1.5	ZEC_{anthro}^{peak}	A/R	2024	2029	2037	
	ZEC_{anthro}^{2100}		2031	2046	2065	
	No cessation		2024	2031	2035	2040
1.7	ZEC_{anthro}^{peak}	A/R	2032	2040	2050	
	ZEC_{anthro}^{2100}		2038	2055	2076	
	No cessation		2031	2039	2044	2052
2.0	ZEC_{anthro}^{peak}		2032	2047	2057	2074
	ZEC_{anthro}^{2100}		2048	2068	N/R	N/R
	No cessation		2040	2052	2061	2077

No cessation, the year in which these temperatures are reached following the emissions scenario without a cessation of emissions; A/R, the temperature commitment has already been reached at that probability level as of the beginning of 2021; N/R, the commitment is not reached at that probability level within the bounds of the experiment (up to year 2080).

of atmospheric CO_2 uptake to global temperatures¹³. An assessment of the effect of different emissions choices on the present-day ZEC_{anthro}^{peak} and ZEC_{anthro}^{2100} is provided in Supplementary Fig. 2.

The 2018 IPCC *Special Report on Global Warming of 1.5°C* concluded that past emissions alone are unlikely (less than 33% probability) to raise global temperature above 1.5°C relative to 1850–1900¹⁴. We find that there is now a 42% probability that the world is committed to peak global warming (ZEC_{anthro}^{peak}) of at least 1.5°C based on past emissions alone and a 2% probability that ZEC_{anthro}^{peak} reaches at least 2.0°C (Fig. 1b). For sustained warming of greater than 1.5°C and 2.0°C at the end of the century (ZEC_{anthro}^{2100}), the probabilities are 5% and 0%, respectively, meaning that society is not yet committed to these levels of long-term warming.

For comparison, we find that a cessation of CO_2 emissions (ZEC_{CO_2}), while holding all other forcings fixed at present-day levels, results in temperatures remaining within approximately 0.1°C of the present-day temperature throughout the century (Fig. 1b, dotted line), consistent with previous studies^{3,8,12}. The end-of-century ZEC_{CO_2} is approximately 0°C (−0.02 to 0.12°C, 66% confidence) relative to present-day temperatures, in good agreement with the AR6 assessed likely range of 0°C ± 0.19°C.

We next consider how ZEC_{anthro}^{peak} and ZEC_{anthro}^{2100} change over time following a range of emissions pathways before cessation, as illustrated by eight SSP emission scenarios: SSP1–1.9, SSP1–2.6, SSP4–3.4, SSP2–4.5, SSP4–6.0, SSP3–7.0-lowNTCF (near-term climate forcing), SSP3–7.0 and SSP5–8.5²⁷. We conduct simulations of the climate response to a cessation of anthropogenic emissions within FaIR in every year for the period 2021–2080 or until CO_2 emissions reach net zero, following each of these SSP scenarios, each run with 6,729 posterior ensemble members (Methods). Figure 2a shows ZEC_{anthro}^{peak} and ZEC_{anthro}^{2100} relative to the pre-industrial period 1850–1900 as a function of the year in which emissions cease along a moderate mitigation scenario (SSP2–4.5) (solid black and dashed black lines, respectively). A key result is that the time at which ZEC_{anthro}^{peak} is reached occurs from four to seven years before that temperature would be exceeded following SSP2–4.5 (horizontal distance between orange and solid black lines and shading in Fig. 2a); while there is a 66% probability of exceeding 1.5°C by 2035, there is a 66% probability of being committed to at least 1.5°C of warming by 2029 (ZEC_{anthro}^{peak} in Fig. 2a; Table 1). For 2°C, this becomes 2061 and 2057, respectively (ZEC_{anthro}^{peak} in Fig. 2a; Table 1). The number of years that ZEC_{anthro}^{peak} is reached before a given warming level is exceeded depends on the probability threshold considered, with the 17th percentile of the ensemble (corresponding to high aerosol forcing and high climate sensitivity) producing a larger difference and the 83rd percentile of the ensemble (corresponding to low aerosol forcing and low climate sensitivity) producing a smaller difference (Table 1).

A similar assessment can be made for ZEC_{anthro}^{2100} , for which temperature thresholds are surpassed after the thresholds themselves are reached in the emissions scenario. We find that the end-of-century warming commitment of 1.5°C occurs by 2055 with 66% probability—15 years after this temperature is reached when following SSP2–4.5 (Fig. 2a)—while the end-of-century warming commitment of 2.0°C is not reached within the bounds of the

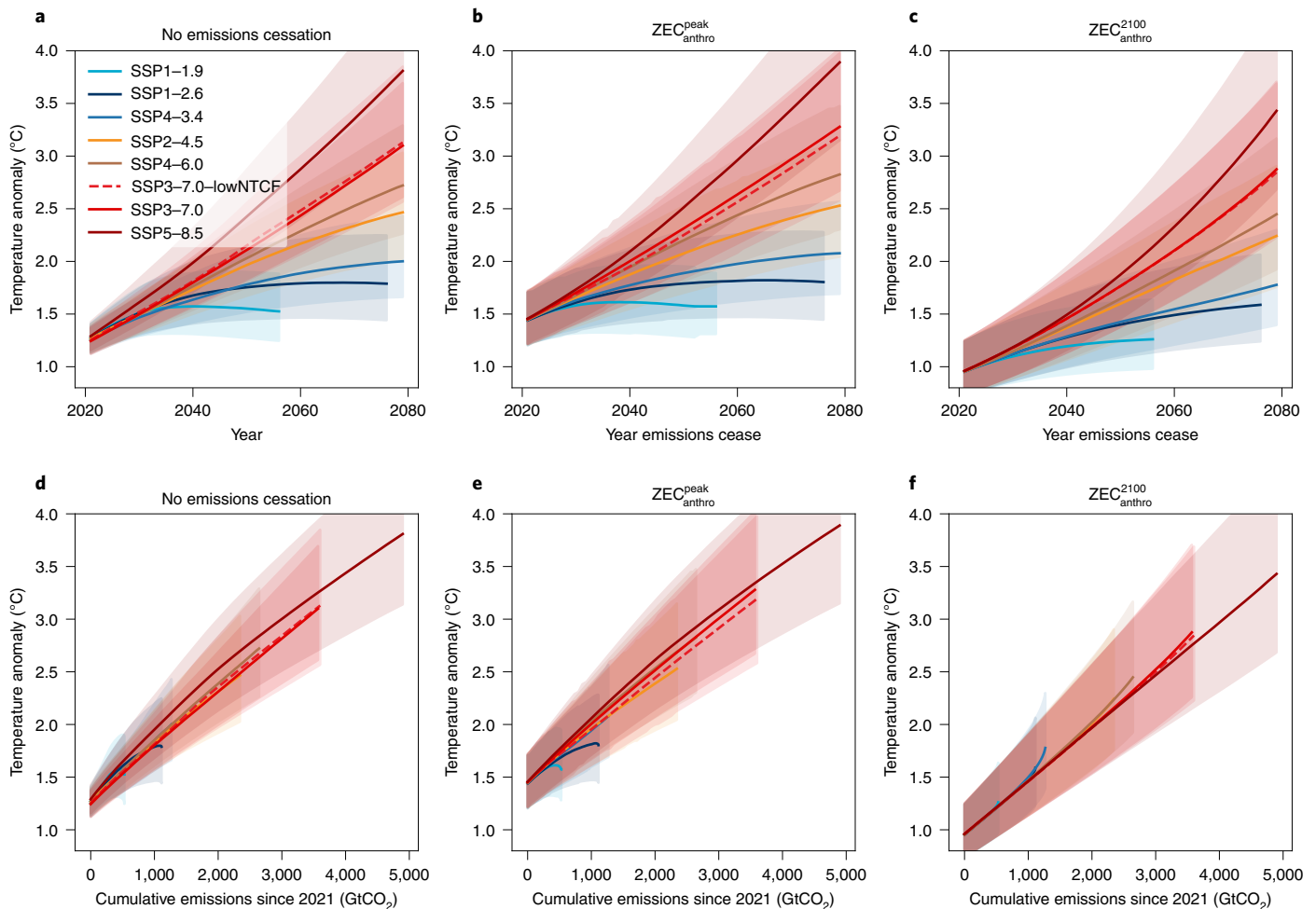


Fig. 3 | Committed warming and scenario warming relative to 1850–1900 for all SSPs. a–c, Temperature response following each SSP with no cessation of emissions as a function of year (**a**), ZEC_{anthro}^{peak} (**b**) and ZEC_{anthro}^{2100} (**c**) as a function of shut-off year until 2080 or when emissions reach net zero. **d–f**, The same as **a–c** but as functions of cumulative emissions since the beginning of 2021. Note that **a**, **b** and **c** correspond to the orange, solid black and dashed black lines presented in Fig. 2, respectively, but for all SSPs. Shading represents the 66% confidence interval.

experiment (by 2080). Since global temperature in 2100 after a cessation of emissions is relatively stable compared with peak warming, this implies that society is not committed to long-term warming of a given magnitude before that temperature is reached following an emissions trajectory.

Considering the seven other emissions scenarios, results show that committed warming of 1.5 and 2 °C (ZEC_{anthro}^{peak}) occurs roughly half a decade before those temperatures would be exceeded if emissions were never halted (Fig. 3a,c,e and Table 1). The choice of emissions pathway becomes increasingly important with time, with high- and very high-emissions scenarios (SSP3–7.0, SSP5–8.5) generating a ZEC_{anthro}^{peak} of 2 °C earlier than lower emissions scenarios. Conversely, only high mitigation (SSP1–1.9, SSP1–2.6) avoids ZEC_{anthro}^{peak} of 2 °C over this century in the 66th percentile. A ZEC_{anthro}^{2100} exceeding 1.5 °C and 2.0 °C following a cessation of emissions in this century is avoided in low- (SSP1–2.6) and in low- to moderate- (SSP4–3.4, SSP2–4.5) emissions scenarios, respectively.

The elevated warming following a cessation of emissions in 2021 (temperature overshoot) lasts 11–48 years (66% confidence range). The length of the temperature overshoot generally declines with aerosol forcing and is therefore dependent on the emissions trajectory; by 2060, a cessation of all emissions along medium- to high-aerosol-forcing scenarios (SSP3–7.0, SSP4–6.0; Fig. E6) results in 6- to 31-year overshoots, while low-aerosol-forcing scenarios

(SSP1–1.9, SSP1–2.6) result in 3- to 10-year overshoots (66% confidence range).

Committed warming as a function of cumulative emissions

The projected twenty-first-century warming following different SSP emissions scenarios (Fig. 3a) simplifies greatly when cast in terms of the cumulative CO₂ emissions (Fig. 3b; calculated as cumulative anthropogenic CO₂ emitted since January 2021). Consistent with previous studies^{28–30}, global warming is nearly proportional to cumulative CO₂ emissions, with small differences between scenarios arising from the assumed rate of emissions and the fractional contribution of non-CO₂ climate forcing to total forcing. A relevant measure of this proportionality is the transient climate response to emissions (TCRE), defined as the global temperature change per 1,000 GtCO₂ emitted. We find that the constrained FaIR ensemble has $TCRE = 0.44$ °C per 1,000 GtCO₂ (0.33–0.59 °C per 1,000 GtCO₂, 66% confidence range) when calculated for SSP2–4.5 for the period 2018–2068 (Supplementary Fig. 4). These estimates are in line with the ref.³¹ estimate of 0.44 °C per 1,000 GtCO₂ (0.32–0.62 °C per 1,000 GtCO₂, 90% range) and the IPCC AR6³² estimate of 0.45 °C per 1,000 GtCO₂ (0.27–0.63 °C per 1,000 GtCO₂, 66% range).

We next evaluate how ZEC_{anthro}^{peak} and ZEC_{anthro}^{2100} scale with the cumulative CO₂ emitted until the year emissions cease. The evolution of ZEC_{anthro}^{peak} is nearly proportional to cumulative CO₂

Table 2 | Estimated remaining carbon budget (GtCO₂) relative to the beginning of 2021 for ZEC^{peak}_{anthro} and ZEC²¹⁰⁰_{anthro} of 1.5, 1.7 and 2 °C following SSP2–4.5 at the 17th, 50th, 66th and 83rd percentile confidence levels

Global warming since 1850–1900 (°C)	Temperature metric	Estimated remaining carbon budget			
		17th	50th	66th	83rd
1.5	ZEC ^{peak} _{anthro}	0	120	340	680
	ZEC ²¹⁰⁰ _{anthro}	420	1,080	1,470	1,870
	No cessation	120	420	600	820
1.7	ZEC ^{peak} _{anthro}	0	470	820	1,260
	ZEC ²¹⁰⁰ _{anthro}	730	1,470	1,830	2,250
	No cessation	420	770	990	1,340
2.0	ZEC ^{peak} _{anthro}	470	1,120	1,550	2,190
	ZEC ²¹⁰⁰ _{anthro}	1,170	1,980	N/R	N/R
	No cessation	820	1,340	1,720	2,280

'No cessation' and 'N/R' are as in Table 1.

emissions (Fig. 3b), despite its dependence on aerosol forcing at the time emissions cease. This is probably due to the approximately constant fraction of aerosol forcing relative to total forcing over time for most individual SSP pathways. Exceptions are SSP1–2.6 and SSP1–1.9, wherein aerosols decrease rapidly during the first half of the twenty-first century and decline more slowly thereafter (Extended Data Fig. 6), resulting in a nonlinear response in peak warming as a function of emissions cessation year. The proportionality with cumulative CO₂ emissions is more evident for ZEC²¹⁰⁰_{anthro}, which is independent of the emissions scenario (Fig. 3c) because the residual CO₂ forcing dominates total forcing by 2100 following a cessation of emissions.

The proportionality of committed warming to cumulative CO₂ emissions permits the quantification of a remaining carbon budget for committed warming of 1.5, 1.7 and 2 °C (Table 2). Total cumulative carbon emitted between 1850 and 2019 is approximately 2,290 GtCO₂, within the IPCC AR6 estimate of 2,390 ± 240 GtCO₂ for the same period³². A median ZEC^{peak}_{anthro} of 1.5 °C is reached after the emission of 120 GtCO₂ (0–340 GtCO₂, 66% confidence) relative to the beginning of 2021 (Fig. 2b); for 2 °C, the remaining carbon budget is 1,120 GtCO₂ (470–1,550 GtCO₂). At the end of the century (ZEC²¹⁰⁰_{anthro}), 1.5 °C is reached after the emission of 1,080 GtCO₂ (420–1,470 GtCO₂); for 2 °C, this remaining carbon budget is 1,980 GtCO₂ (1,170 GtCO₂—not reached within the experiments). Uncertainty in the remaining carbon budgets stems mainly from uncertainties in aerosol forcing and climate sensitivity. However, the results are consistent across the emissions scenarios (Supplementary Table 2)—a key to maintaining consistency in the calculation of carbon budgets³¹.

Remaining carbon budgets estimated using the ZEC can be contrasted with those estimated following emissions pathways without a cessation of emissions (Table 2). In the latter case, 1.5 °C is exceeded with 66% probability when cumulative emissions since 2021 reach 600 GtCO₂ following SSP2–4.5 (orange line in Fig. 2b), a measure of the 'threshold exceedance budget'³². This is substantially larger than the 66th percentile estimate of 340 GtCO₂ using ZEC^{peak}_{anthro} because it does not account for the additional warming that would occur as aerosol forcing is reduced upon abrupt cessation of emissions. The smaller carbon budgets obtained using ZEC^{peak}_{anthro} would provide an underestimate for emissions pathways that achieve net-zero CO₂ through the implementation of CO₂ removal technologies while maintaining some level of anthropogenic aerosol emissions.

However, compared with scenarios that phase out emissions more slowly and without net-negative CO₂, ZEC^{peak}_{anthro} provides the smallest estimate of peak warming over the twenty-first century and therefore can be considered a lower bound on committed warming (Extended Data Fig. 7).

These calculations are relatively pathway independent across priority SSPs and are therefore robust to choice of emissions trajectory. As such, they do not require an examination of only a subset of emissions trajectories that are calibrated to avoid 1.5 or 2 °C (such as those presented in IPCC AR6) or that are constrained by socio-economic feasibility^{14,33}. This methodology is appropriate when considering the possibility of a temperature overshoot that may persist for over a decade, with subsequent impacts on human and natural systems that respond quickly, and perhaps irreversibly, to global warming.

Two important insights are that (1) the world will have a greater than 66% probability of being committed to peak warming above 1.5 °C by 2027–2032 in all emissions scenarios and 2 °C by 2043–2057 in medium- to high-emissions scenarios (SSP2–4.5 to SSP5–8.5), and (2) these temperature commitments will occur four to six years before the 1.5 and 2 °C warming levels will be exceeded, assuming emissions follow SSP2–4.5. We find that the 1.5 and 2.0 °C peak warming commitments (ZEC^{peak}_{anthro}) correspond to median carbon budgets of approximately 120 and 1,120 GtCO₂ relative to the beginning of 2021, respectively. Given that FaIR does not capture the possibility of future destabilizing climate feedbacks such as decreased ice-sheet cover³⁴, thawing permafrost and methane hydrate dissociation due to ocean warming^{35,36} or a sea surface temperature pattern effect that allows for a more substantial shift towards destabilizing cloud feedbacks in the future than modelled here^{10,37–40}, these estimates of the timing of geophysical warming commitments may become underestimates as global temperatures rise.

Online content

Any methods, additional references, Nature Research reporting summaries, source data, extended data, supplementary information, acknowledgements, peer review information; details of author contributions and competing interests; and statements of data and code availability are available at <https://doi.org/10.1038/s41558-022-01372-y>.

Received: 14 October 2021; Accepted: 25 April 2022;

Published online: 6 June 2022

References

- Lee, J.-Y. et al. in *Climate Change 2021: The Physical Science Basis* (eds Masson-Delmotte, V. et al.) Ch. 4 (IPCC, Cambridge Univ. Press, 2021).
- Solomon, S., Plattner, G.-K., Knutti, R. & Friedlingstein, P. Irreversible climate change due to carbon dioxide emissions. *Proc. Natl. Acad. Sci. USA* **106**, 1704–1709 (2009).
- Armour, K. C. & Roe, G. H. Climate commitment in an uncertain world. *Geophys. Res. Lett.* <https://doi.org/10.1029/2010GL045850> (2011).
- Ehler, D. & Zickfeld, K. What determines the warming commitment after cessation of CO₂ emissions? *Environ. Res. Lett.* **12**, 015002 (2017).
- Goodwin, P., Williams, R. G. & Ridgwell, A. Sensitivity of climate to cumulative carbon emissions due to compensation of ocean heat and carbon uptake. *Nat. Geosci.* **8**, 29–34 (2015).
- Williams, R. G., Roussenov, V., Frölicher, T. L. & Goodwin, P. Drivers of continued surface warming after cessation of carbon emissions. *Geophys. Res. Lett.* **44**, 10633–10642 (2017).
- Frölicher, T. L., Winton, M. & Sarmiento, J. L. Continued global warming after CO₂ emissions stoppage. *Nat. Clim. Change* **4**, 40–44 (2014).
- MacDougall, A. H. et al. Is there warming in the pipeline? A multi-model analysis of the zero emissions commitment from CO₂. *Biogeosciences* **17**, 2987–3016 (2020).
- Winton, M., Takahashi, K. & Held, I. M. Importance of ocean heat uptake efficacy to transient climate change. *J. Clim.* **23**, 2333–2344 (2010).
- Zhou, C., Zelinka, M. D., Dessler, A. E. & Wang, M. Greater committed warming after accounting for the pattern effect. *Nat. Clim. Change* **11**, 132–136 (2021).

11. Hare, B. & Meinshausen, M. How much warming are we committed to and how much can be avoided? *Climatic Change* **75**, 111–149 (2006).
12. Mauritsen, T. & Pincus, R. Committed warming inferred from observations. *Nat. Clim. Change* **7**, 652–655 (2017).
13. Smith, C. J. et al. Current fossil fuel infrastructure does not yet commit us to 1.5°C warming. *Nat. Commun.* **10**, 101 (2019).
14. Allen, M. et al. Technical Summary. In *Special Report on Global Warming of 1.5°C* (eds Masson-Delmotte, V. et al.) (IPCC, WMO, 2018).
15. Matthews, H. & Zickfeld, K. Climate response to zeroed emissions of greenhouse gases and aerosols. *Nat. Clim. Change* **2**, 338–341 (2012).
16. Chen, D. et al. in *Climate Change 2021: The Physical Science Basis* (eds Masson-Delmotte, V. et al.) Ch. 1 (IPCC, Cambridge Univ. Press, 2021).
17. von Schuckmann, K. et al. Heat stored in the Earth system: where does the energy go? *Earth Syst. Sci. Data* **12**, 2013–2041 (2020).
18. Forster, P. et al. in *Climate Change 2021: The Physical Science Basis* (eds Masson-Delmotte, V. et al.) Ch. 7 (IPCC, Cambridge Univ. Press, 2021).
19. Bellouin, N. et al. Bounding global aerosol radiative forcing of climate change. *Rev. Geophys.* **58**, e2019RG000660 (2020).
20. Sherwood, S. C. et al. An assessment of Earth's climate sensitivity using multiple lines of evidence. *Rev. Geophys.* **58**, e2019RG000678 (2020).
21. Smith, C. J. et al. FAIR v1.3: a simple emissions-based impulse response and carbon cycle model. *Geosci. Model Dev.* **11**, 2273–2297 (2018).
22. Millar, R. J., Nicholls, Z. R., Friedlingstein, P. & Allen, M. R. A modified impulse–response representation of the global near-surface air temperature and atmospheric concentration response to carbon dioxide emissions. *Atmos. Chem. Phys.* **17**, 7213–7228 (2017).
23. Jones, C. D., Frolicher, T. M. & Koven, C. The Zero Emissions Commitment Model Intercomparison Project (ZECMIP) contribution to C4MIP: quantifying committed climate changes following zero carbon emissions. *Geosci. Model Dev.* **12**, 4375–4385 (2019).
24. Held, I. M. et al. Probing the fast and slow components of global warming by returning abruptly to preindustrial forcing. *J. Clim.* **23**, 2418–2427 (2010).
25. Geoffroy, O. et al. Transient climate response in a two-layer energy-balance model. Part I: analytical solution and parameter calibration using CMIP5 AOGCM experiments. *J. Clim.* **26**, 1841–1857 (2013).
26. Smith, C. et al. in *Climate Change 2021: The Physical Science Basis* (eds Masson-Delmotte, V. et al.) Ch. 7 Supplementary Material (IPCC, Cambridge Univ. Press, 2021).
27. Riahi, K., van Vuuren, D. P. & Kriegler, E. et al. The Shared Socioeconomic Pathways and their energy, land use, and greenhouse gas emissions implications: an overview. *Glob. Environ. Change* **42**, 153–168 (2017).
28. Allen, M. R. et al. Warming caused by cumulative carbon emissions towards the trillionth tonne. *Nature* **458**, 1163–1166 (2009).
29. Matthews, H. D., Gillett, N. P., Stott, P. A. & Zickfeld, K. The proportionality of global warming to cumulative carbon emissions. *Nature* **459**, 829–832 (2009).
30. MacDougall, A. H. & Friedlingstein, P. The origin and limits of the near proportionality between climate warming and cumulative CO₂ emissions. *J. Clim.* **28**, 4217–4230 (2015).
31. Matthews, H. D. et al. Opportunities and challenges in using remaining carbon budgets to guide climate policy. *Nat. Geosci.* **13**, 769–779 (2020).
32. Canadell, J. G. et al. in *Climate Change 2021: The Physical Science Basis* (eds Masson-Delmotte, V. et al.) Ch. 5 (IPCC, Cambridge Univ. Press, 2021).
33. Rogelj, J., Forster, P. M., Kriegler, E., Smith, C. J. & Séférian, R. Estimating and tracking the remaining carbon budget for stringent climate targets. *Nature* **571**, 335–342 (2019).
34. Goosse, H. et al. Quantifying climate feedbacks in polar regions. *Nat. Commun.* **9**, 1919 (2018).
35. MacDougall, A. H. Estimated effect of the permafrost carbon feedback on the zero emissions commitment to climate change. *Biogeosciences* **18**, 4937–4952 (2021).
36. Ruppel, C. D. & Kessler, J. D. The interaction of climate change and methane hydrates. *Rev. Geophys.* **55**, 126–168 (2017).
37. Andrews, T. et al. Accounting for changing temperature patterns increases historical estimates of climate sensitivity. *Geophys. Res. Lett.* **45**, 8490–8499 (2018).
38. Silvers, L. G., Paynter, D. & Zhao, M. The diversity of cloud responses to twentieth century sea surface temperatures. *Geophys. Res. Lett.* **45**, 391–400 (2018).
39. Zhou, C., Zelinka, M. D. & Klein, S. A. Impact of decadal cloud variations on the Earth's energy budget. *Nat. Geosci.* **9**, 871–874 (2016).
40. Zhou, C., Zelinka, M. D. & Klein, S. A. Analyzing the dependence of global cloud feedback on the spatial pattern of sea surface temperature change with a Green's function approach. *J. Adv. Model. Earth Syst.* **9**, 2174–2189 (2017).
41. Morice, C. P., Kennedy, J. J., Rayner, N. A. & Jones, P. D. Quantifying uncertainties in global and regional temperature change using an ensemble of observational estimates: the HadCRUT4 data set. *J. Geophys. Res. Atmos.* <https://doi.org/10.1029/2011JD017187> (2012).

Publisher's note Springer Nature remains neutral with regard to jurisdictional claims in published maps and institutional affiliations.

© The Author(s), under exclusive licence to Springer Nature Limited 2022

Methods

Model. We use FaIR v.1.3.6²¹ for all historical and future climate simulations. Historical simulations are run using the Reduced-Complexity Model Intercomparison Project-generated SSP emissions time series for the period 1765–2016; future scenarios are run for SSP1–1.9, SSP1–2.6, SSP4–3.4, SSP2–4.5, SSP4–6.0, SSP3–7.0-lowNTCF, SSP3–7.0 and SSP5–8.5 for the period 2016–2100, with an abrupt cessation of all anthropogenic emissions in every year along each pathway until 2080 or until CO₂ emissions reach net zero; CO₂ emissions are set to zero while all other emissions are set to pre-industrial (1765) levels to retain background sources. Background emissions of N₂O and CH₄ for the historical period and into the future are prescribed using the default time series in FaIR, where emissions vary over the historical period but are constant from 2005 onwards as a proxy for natural sources.

Forcing associated with land-use change is not included over the historical record or in future projections due to the lack of a dynamic vegetation model and its overestimation in FaIR relative to AR6 estimates¹⁸. Land-use change associated with the zero-emissions commitment was also not modelled in intermediate-complexity models participating in the Zero Emissions Commitment Model Intercomparison Project (ZECMIP)²³. Including land-use forcing does not substantially change the results (Supplementary Fig. 1). To isolate anthropogenic warming, volcanic and solar forcing are not included in future emissions scenarios. Volcanic forcing for the historical period is scaled by a factor of 0.6 to obtain better agreement with historical aerosol forcing and global temperatures (similar scaling down of volcanic efficacy has previously been performed in the Model for the Assessment of Greenhouse Gas Induced Climate Change (MAGICC) for better correspondence to observed temperatures²⁴).

We modify FaIR to use the ref.²⁴ two-layer energy balance model to calculate global temperatures from radiative forcing. The equations for this energy balance model are:

$$C \frac{dT}{dt} = F + \lambda T - \epsilon \gamma (T - T_0)$$

$$C_0 \frac{dT_0}{dt} = \gamma (T - T_0)$$

where C and C_0 are, respectively, the heat capacities of the first layer (representing the surface components of the climate system, including the atmosphere, land, sea ice and ocean mixed layer) and second layer (representing the deep ocean); γ is the coefficient of heat exchange between the two layers, representing a measure of the ocean heat uptake efficiency; λ is the radiative feedback parameter; and ϵ is a deep ocean efficacy factor that expresses the time dependence of the global radiative feedback (see refs. 24,25). The equilibrium climate sensitivity is given by

$$\text{ECS} = -\frac{F_{2x}}{\lambda}$$

where F_{2x} is the forcing for CO₂ doubling. Retaining the two-layer energy balance model in FaIR allows us to diagnose heat uptake, account for feedback time dependence and model feedback parameters estimated from general circulation models²⁵.

Ensemble development. A 300,000-member FaIR ensemble is generated by drawing random values from prior probability distributions of ECS (uniform from 1 to 6°C), ocean model variables and carbon-cycle parameters. Normal prior distributions of γ , C and C_0 are generated using distributions from global climate models²⁵ but with standard deviations (σ) expanded by 50%; the distribution in γ is truncated to avoid values less than 0.1, while C_0 is truncated to avoid sampling deep ocean heat capacities less than 10 W m⁻² °C⁻¹ yr⁻¹ (γ : mean = 0.67 W m⁻² °C⁻¹, σ = 0.225 W m⁻² °C⁻¹; C : mean = 8.2 W m⁻² °C⁻¹ yr⁻¹, σ = 1.4 W m⁻² °C⁻¹ yr⁻¹; C_0 : mean = 124.7 W m⁻² °C⁻¹ yr⁻¹, σ = 65.8 W m⁻² °C⁻¹ yr⁻¹). A lognormal prior distribution for ϵ is generated using distributions from global climate models²⁵ (mean = 1.28, σ = 0.375), with values of ϵ above unity reflecting the fact that the effective climate sensitivity is expected to become larger in the future as the geographic pattern of warming changes on timescales of multiple centuries^{18,43–45}.

We scale GHG forcing due to CO₂, CH₄ and N₂O in every year by a constant amount generated from normal distributions that match the updated IPCC AR6 ‘very likely’ range (90% confidence interval) of radiative forcing over the industrial period (1750–2018; CO₂: mean = 2.15 W m⁻², σ = 0.16 W m⁻²; CH₄: mean = 0.54 W m⁻², σ = 0.07 W m⁻²; N₂O: mean = 0.19 W m⁻², σ = 0.02 W m⁻²). Aerosol forcing is also scaled by a constant amount by values drawn from a uniform distribution ranging from –2.2 to –0.1 W m⁻² to adequately sample the full range of possible forcing values. All other gases and short-lived climate forcers are treated using default parameterizations in FaIR (not scaled).

Uncertainty in FaIR carbon-cycle parameters associated with various uptake processes is treated as in refs. 13,21. Because FaIR has no representation of internal variability, ZEC_{anthro}^{peak} and ZEC_{anthro}²¹⁰⁰ are quantified on the basis of annual mean temperature values.

Constraining the model. Following the methods of ref. 46, a Bayesian framework is used to constrain model outputs to observational estimates of global mean sea surface temperature (T), ocean heat uptake (Q) and radiative forcing (F) for the 2006–2019 mean relative to the 1850–1900 baseline, reducing the model ensemble to 6,729 members. Specifically, only ensemble members that satisfy the condition:

$$\sqrt{\left(\frac{\delta T}{\sigma_T}\right)^2 + \left(\frac{\delta Q}{\sigma_Q}\right)^2 + \left(\frac{\delta F}{\sigma_F}\right)^2} < 1.65$$

are kept, where δT , δQ and δF are the differences between the model-derived estimates of global surface temperature, ocean heat uptake and total radiative forcing anomalies (2006–2019 mean relative to the 1850–1900 baseline) and observational estimates, with σ_T , σ_Q and σ_F representing one standard deviation of the mean for each of these values and 1.65 corresponding to the 90% confidence level. Observational values are taken from the IPCC AR6: $\Delta T_{\text{obs}} = 1.03 \pm 0.2$ °C, $\Delta Q_{\text{obs}} = 0.59 \pm 0.35$ W m⁻² and $\Delta F_{\text{obs}} = 2.20 \pm 0.7$ W m⁻² (ref. 18), where Δ refers to changes between the two time periods. Modelled CO₂ concentrations are additionally constrained to be within ± 2 ppm of the 2006–2018 mean (395.98 ppm)⁴⁷.

This method produces a posterior estimate on the equilibrium climate sensitivity of 2.9 °C (1.8–4.7 °C), which is consistent with the most recent estimate of 2.3–4.7 °C provided by ref. 20 and 2–5 °C as assessed in IPCC AR6. Posterior estimates of aerosol forcing and the remaining four free parameters in the two-layer ocean model (γ , ϵ , C and C_0) are shown in Extended Data Figs. 1–4). However, the observational record is not long enough to adequately constrain ϵ owing to the slow adjustment of the deep ocean (the timescale on which the value of ϵ becomes relevant for surface warming). The posterior distribution of ϵ used in this study is thus the same as the prior (Extended Data Fig. 2c); however, sensitivity tests show that the choice of prior distribution in ϵ does not substantially affect the conclusions presented here (Supplementary Fig. 3).

Data availability

All data necessary to interpret, verify and extend the research in this article are available to download from the online repository Zenodo⁴⁸.

Code availability

The FaIR model is available to download from the public code repository GitHub (<https://github.com/OMS-NetZero/FAIR>). All other code used to set up model simulations, analyse model output and create figures are available to view and download from GitHub⁴⁹.

References

- Meinshausen, M. et al. The RCP greenhouse gas concentrations and their extensions from 1765 to 2300. *Climatic Change* **109**, 213 (2011).
- Andrews, T., Gregory, J. M. & Webb, M. J. The dependence of radiative forcing and feedback on evolving patterns of surface temperature change in climate models. *J. Clim.* **28**, 1630–1648 (2015).
- Dong, Y., Proistosescu, C., Armour, K. C. & Battisti, D. S. Attributing historical and future evolution of radiative feedbacks to regional warming patterns using a Green's function approach: the preeminence of the western Pacific. *J. Clim.* **32**, 5471–5491 (2019).
- Dong, Y. et al. Intermodel spread in the pattern effect and its contribution to climate sensitivity in CMIP5 and CMIP6 models. *J. Clim.* **33**, 7755–7775 (2020).
- Armour, K. C. Energy budget constraints on climate sensitivity in light of inconstant climate feedbacks. *Nat. Clim. Change* **7**, 331–335 (2017).
- Trends in Atmospheric Carbon Dioxide: Mauna Loa CO₂ Annual Mean Data* (NOAA, 2020); https://gml.noaa.gov/webdata/ccgg/trends/co2/co2_annmean_mlo.txt
- Dvorak, M. Data for ‘Estimating the timing of geophysical commitment to 1.5 and 2.0 °C’. Zenodo <https://doi.org/10.5281/zenodo.6456363> (2022).
- Dvorak, M. michelledvorak/climate: Methods for ‘Estimating the timing of geophysical commitment to 1.5 and 2.0 °C’ (Version v1). Zenodo <https://doi.org/10.5281/zenodo.6455705> (2022).

Acknowledgements

The authors acknowledge funding from the following sources: National Science Foundation Grant AGS-1752796 (M.T.D., K.C.A.), Alfred P. Sloan Research Fellowship FG-2020-13568 (K.C.A.), NOAA Grant UWSC12184 (C.P.), NERC/IIASA Collaborative Research Fellowship NE/T009381/1 (C.J.S.) and NSF grant AGS-1665247 (D.M.W.F.).

Author contributions

M.T.D., K.C.A. and C.P. designed the study. M.T.D. performed the analysis. K.C.A., C.P., D.M.W.F., M.B.B. and C.J.S. made suggestions to the analysis and helped interpret the results. M.T.D. wrote the manuscript with edits from all other authors.

Competing interests

The authors declare no competing interests.

Additional information

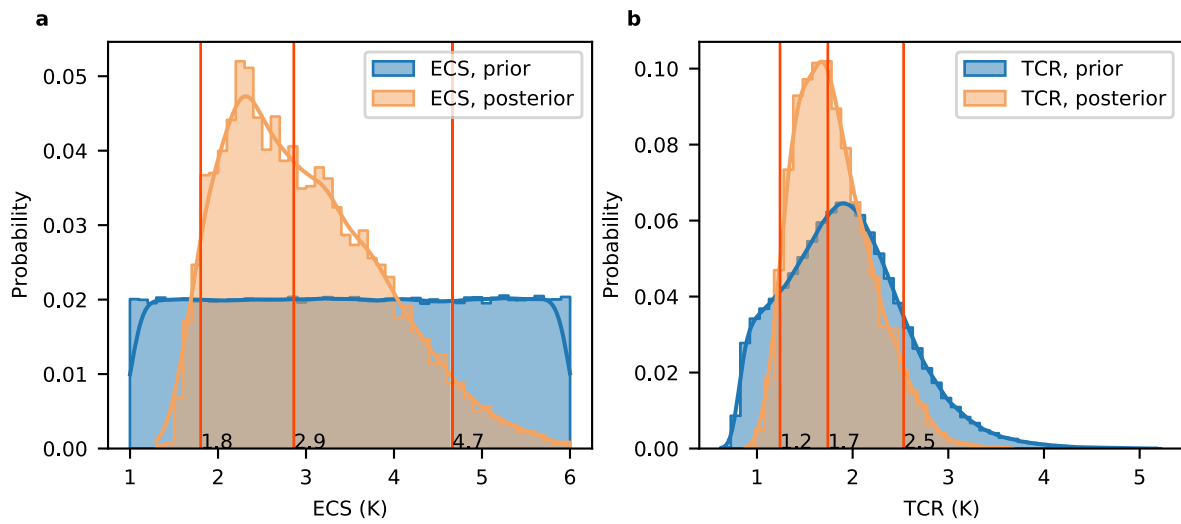
Extended data is available for this paper at <https://doi.org/10.1038/s41558-022-01372-y>.

Supplementary information The online version contains supplementary material available at <https://doi.org/10.1038/s41558-022-01372-y>.

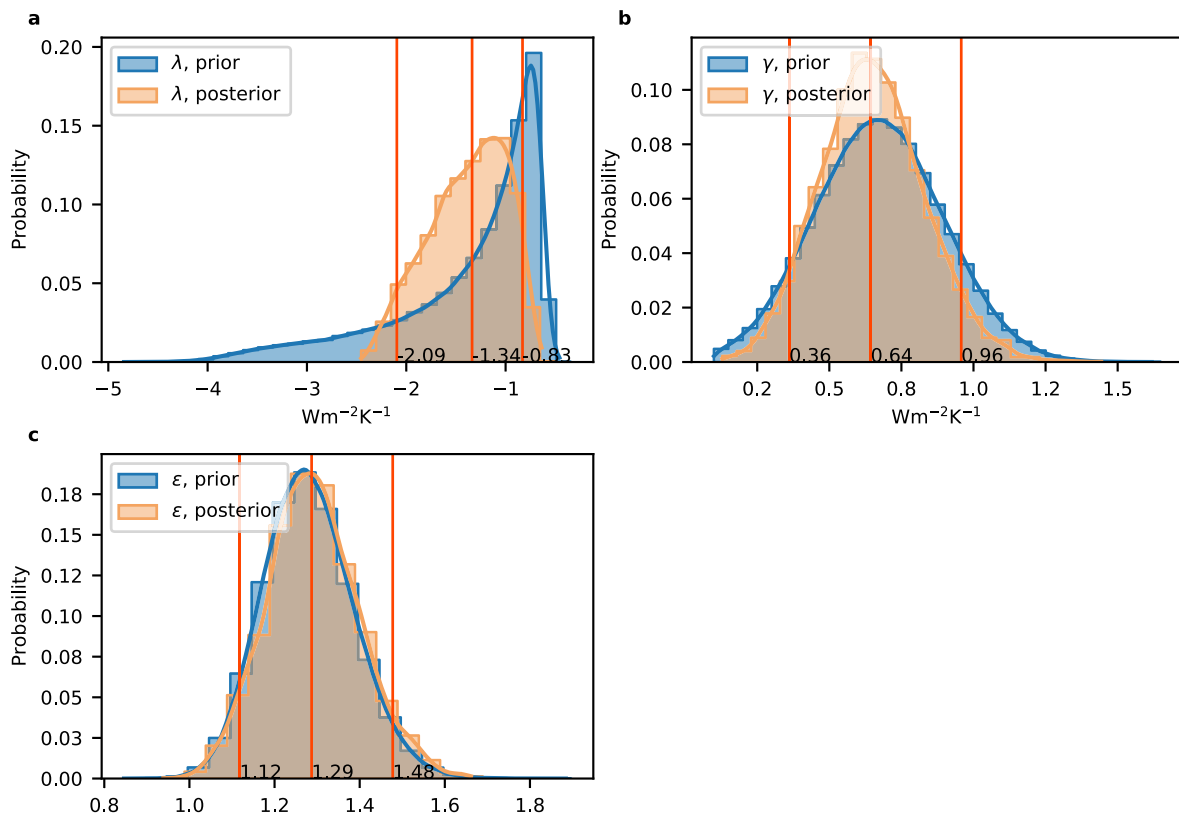
Correspondence and requests for materials should be addressed to M. T. Dvorak.

Peer review information *Nature Climate Change* thanks Chris Jones, Andrew MacDougall and Alexander MacIsaac for their contribution to the peer review of this work.

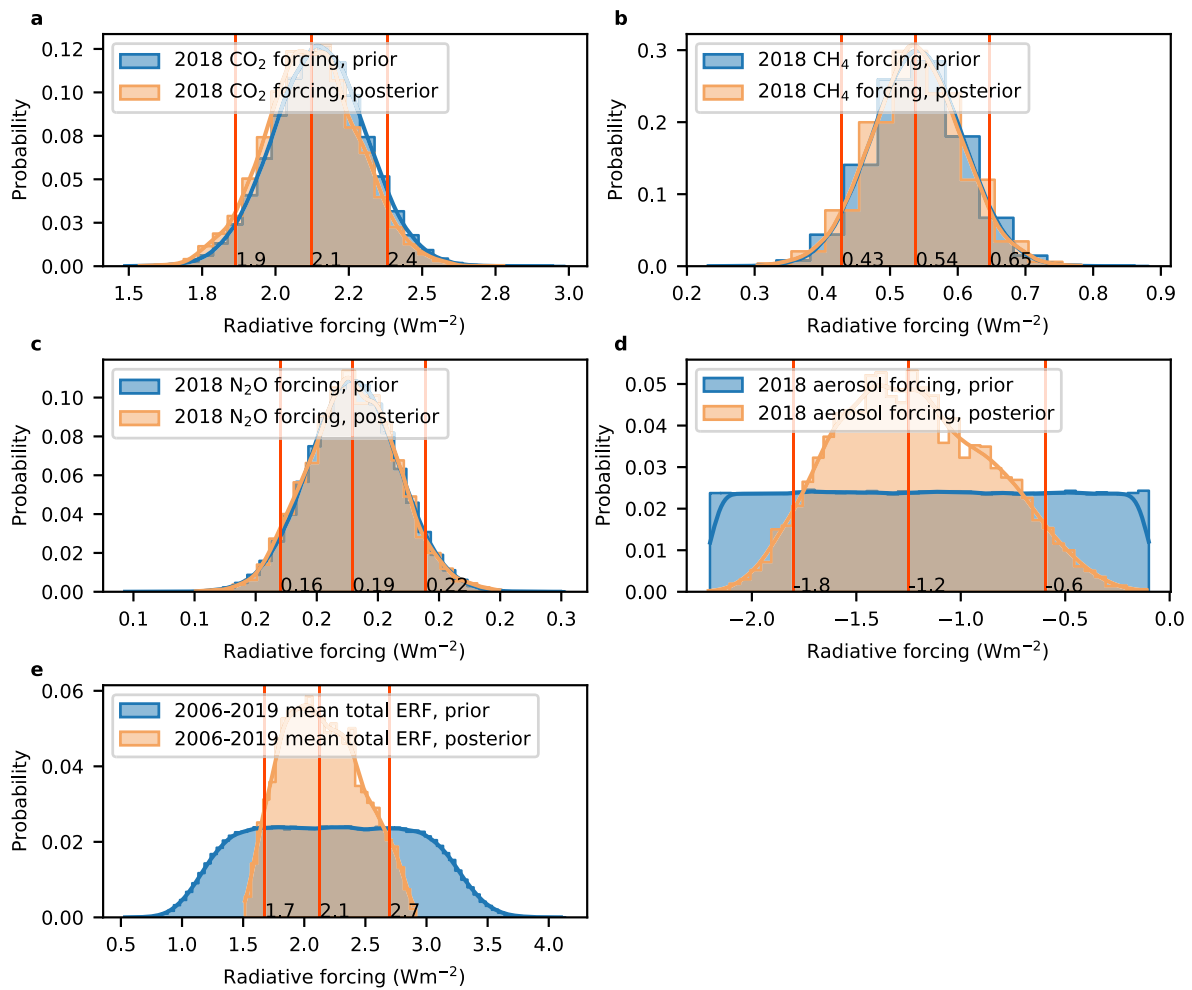
Reprints and permissions information is available at www.nature.com/reprints.



Extended Data Fig. 1 | Prior and posterior distributions of climate response metrics. Posterior estimates of ECS (a) and TCR (b) are 2.9°C [1.8-4.7°C, 90% confidence] and 1.7°C [1.2-2.5°C], respectively.

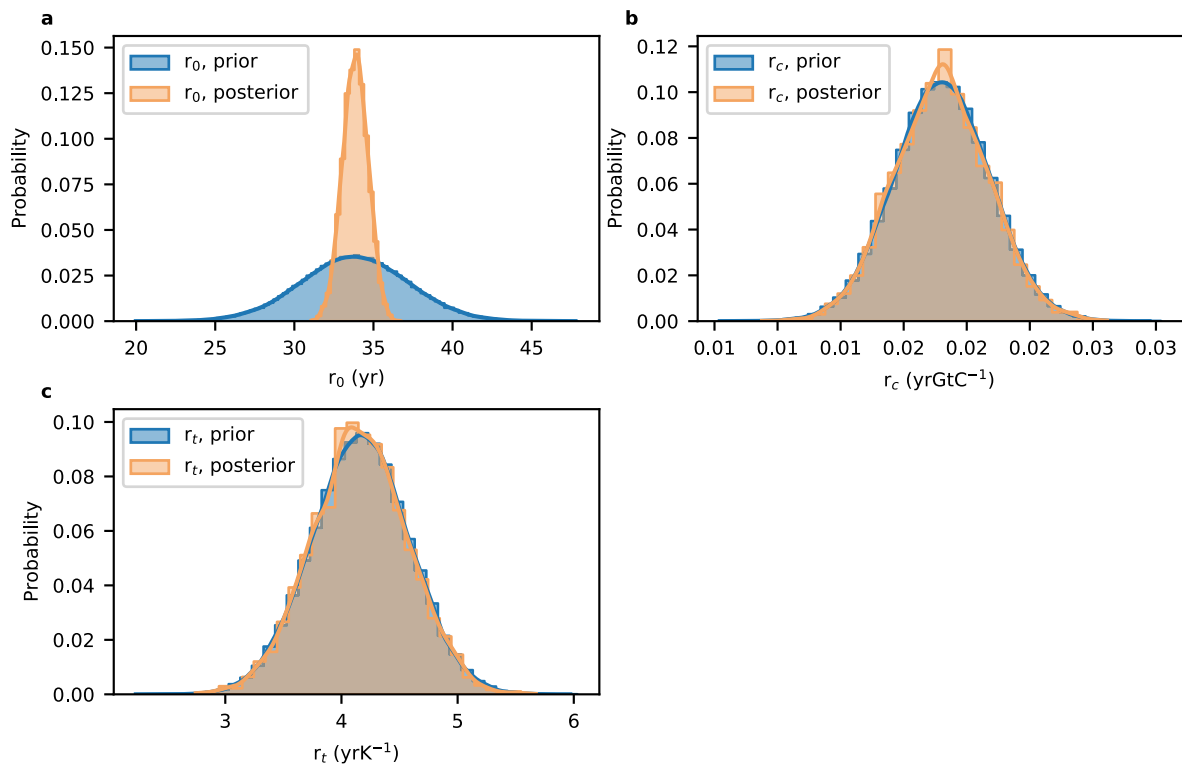


Extended Data Fig. 2 | Prior and posterior distributions of Held two-layer model variables. The global radiative feedback parameter, λ (**a**), ocean heat exchange coefficient, γ (**b**), and deep ocean efficacy factor, ϵ (**c**). Note that neither γ nor ϵ are well constrained by the observational record. See Supplementary Figure S3 for a sensitivity test of the effect of uncertainty in these variables on results.

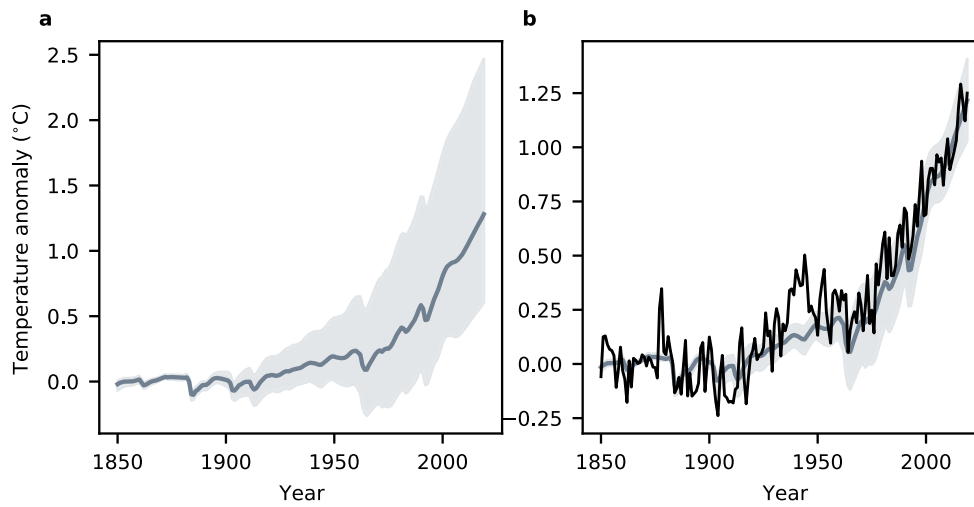


Extended Data Fig. 3 | Prior and posterior distributions of radiative forcing for main GHGs and aerosols, with the 5th, 50th and 95th percentiles indicated.

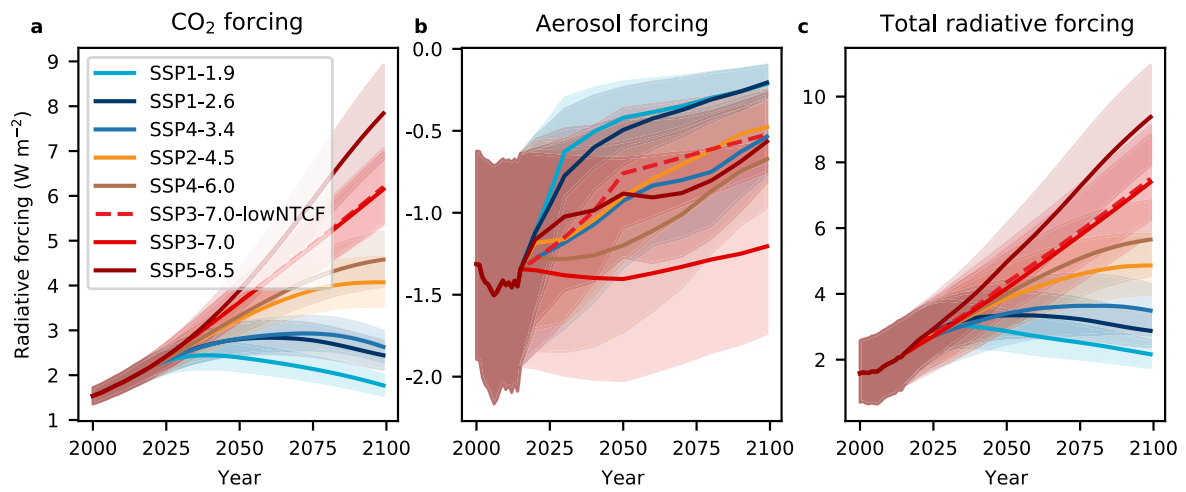
CO_2 (a), CH_4 (b), N_2O (c), and aerosol (d) forcing in 2018 relative to 1765. Total ERF (e) is the 2006-2019 mean relative to the 1850-1900 average. Note that the posterior median total ERF of 2.1 Wm^{-2} corresponds well with the observational value of 2.2 Wm^{-2} , $\sigma = 0.43 \text{ Wm}^{-2}$. Median aerosol forcing agrees well with the AR6 estimate of -1.1 Wm^{-2} [-2.0 to -0.4 Wm^{-2}] for the same period.



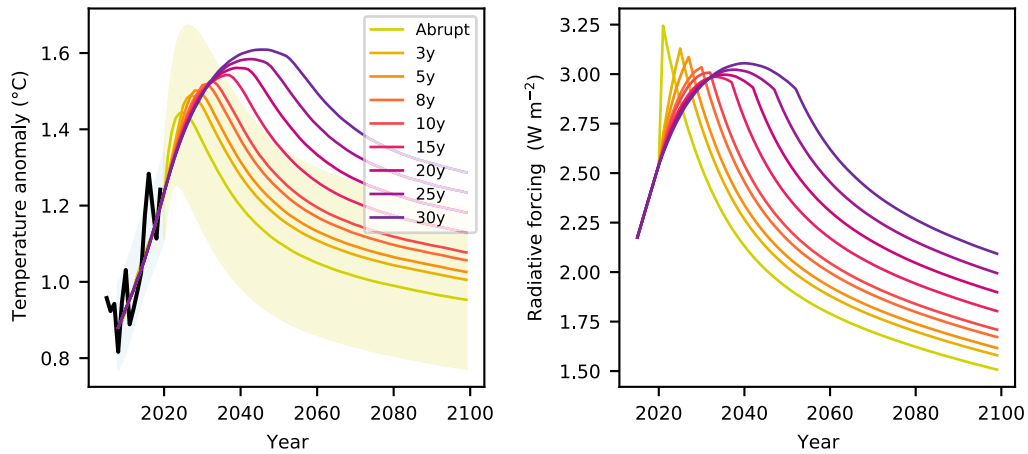
Extended Data Fig. 4 | Prior and posterior distributions of carbon cycling parameters. R_0 (a) represents the airborne fraction of CO_2 during the preindustrial, and r_t (b) and r_c (c) capture the decreasing absorption efficacy of land and ocean carbon sinks with rising global temperatures and CO_2 concentrations, respectively. Note that r_c and r_t are not well-constrained by the observational record. The posterior mean r_0 is 33.8 years, which is between that of Millar et al.'s (2017) value of 32.4 years, and Smith et al.'s (2018) value of 35 years.



Extended Data Fig. 5 | Observational constraint results in a closer reproduction of the historical temperature record from 1850-2020 relative to 1850-1900. Prior (300,000 member) (**a**) and posterior (6,729) (**b**) modeled global temperatures. The observed temperature (overlaid in black) is the ensemble mean from the HadCRUT5 blended air and sea surface temperature dataset (⁴⁹). Shading represents the 90% confidence interval.



Extended Data Fig. 6 | Modeled radiative forcing for the period 2000-2100 relative to 1765 for each SSP scenario. CO₂ (a), Aerosol (b), and total (c) radiative forcing. Shading represents the 90% confidence interval.



Extended Data Fig. 7 | Abrupt emissions cessation results in less warming relative to linear phase-out scenarios. Modeled global temperature anomaly relative to 1850-1900 (**a**) and total radiative forcing relative to 1765 (**b**) for a phase-out of anthropogenic emissions as compared to the abrupt cessation shown in the main paper ('abrupt') following SSP2-4.5. Legend indicates the number of years over which the phase-out occurred, beginning in 2021, where emissions of all gases decrease linearly to zero (GHGs) and to 1765 levels (all other gases), with no net-negative CO_2 emissions.